

Applications of a deep convolutional autoencoder to process pulses from a p-type point contact germanium detector

CAP Congress 2023 | Fredericton, NB

Mark Anderson

anderson.mark@queensu.ca

June 19th, 2023

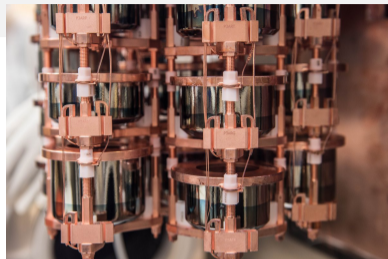


Canadian Association
of Physicists

Association canadienne
des physiciens et physiciennes

Introduction

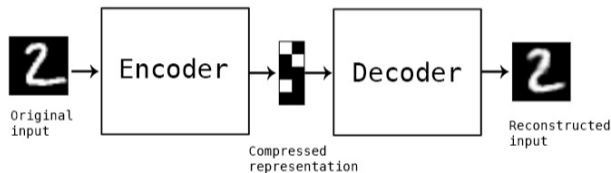
- High-purity germanium (HPGe) detectors widely used in beyond Standard Model rare event searches ($0\nu\beta\beta$, dark matter, etc.)^[2,3,4,5,6,7,8,9]
- Electronic noise makes signal identification challenging
 - Rare events in the presence of backgrounds
- Noise removal could help advance these searches
 - Identify low-energy signal events that would otherwise be dominated by electronic noise
 - Improved background rejection based on pulse shapes
 - More accurate measurements of pulse amplitudes → better energy resolution
- Deep learning has been successfully used in other fields (typically 2D images)
 - Why not 1D pulses from HPGe detectors?



[10]

Autoencoders

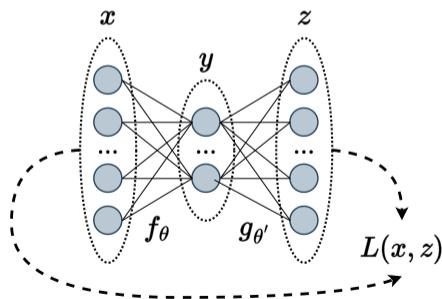
- An autoencoder is an algorithm used to learn a useful representation of data
 - Trained to map the inputs to the inputs (with some form of constraint)



- By definition, an autoencoder is *lossy*
 - The goal is to retain as much *useful* information as possible
- Typically a (deep) neural network

Denosing autoencoders

- Denoising autoencoders impose the constraint that reconstruction must also remove noise
 - Proposed as a method to extract robust features for other classification tasks^[12]
 - Input becomes a corrupted version of x , \tilde{x} , by some process $q_{\mathcal{D}}$



Internal/latent representation, y :

$$f_{\theta}(x) = y$$

Input reconstruction, z :

$$g_{\theta'}(y) = g_{\theta'}(f_{\theta}(x)) = z$$

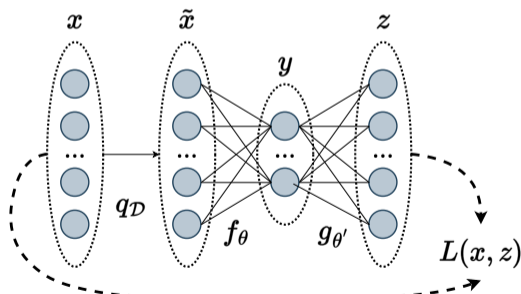
Minimize some **loss function** quantifying the reconstruction of x , $L(x, z)$

$$L(x, z) = \frac{1}{N} \sum_i \|z_i - x_i\|_2^2$$

[1]

Denosing autoencoders

- Denoising autoencoders impose the constraint that reconstruction must also remove noise
 - Proposed as a method to extract robust features for other classification tasks^[12]
 - Input becomes a corrupted version of x , \tilde{x} , by some process $q_{\mathcal{D}}$



Internal/latent representation, y :

$$f_{\theta}(\tilde{x}) = y$$

Input reconstruction, z :

$$g_{\theta'}(y) = g_{\theta'}(f_{\theta}(\tilde{x})) = z$$

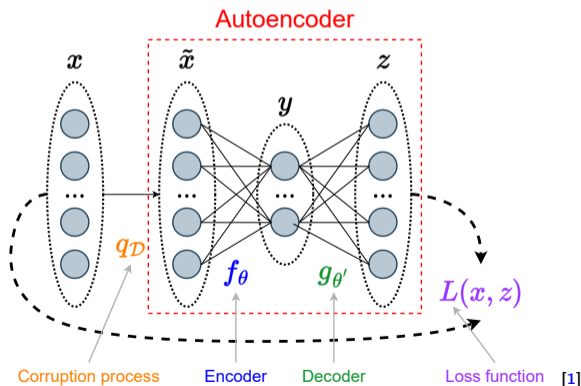
Minimize some **loss function** quantifying the reconstruction of x , $L(x, z)$

$$L(x, z) = \frac{1}{N} \sum_i^N \|z_i - x_i\|_2^2$$

[1]

Denosing autoencoders

- Denoising autoencoders impose the constraint that reconstruction must also remove noise
 - Proposed as a method to extract robust features for other classification tasks^[12]
 - Input becomes a corrupted version of x , \tilde{x} , by some process $q_{\mathcal{D}}$



Internal/latent representation, y :

$$f_{\theta}(\tilde{x}) = y$$

Input reconstruction, z :

$$g_{\theta'}(y) = g_{\theta'}(f_{\theta}(\tilde{x})) = z$$

Minimize some **loss function** quantifying the reconstruction of x , $L(x, z)$

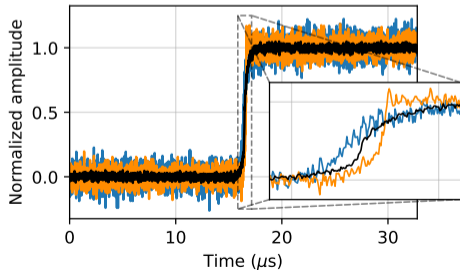
$$L(x, z) = \frac{1}{N} \sum_i^N \|z_i - x_i\|_2^2$$

The detector

- Signals are from a 1 kg p-type point contact detector located at Queen's University
 - Cylindrical with a radius of 3 cm and height of 5 cm
 - Manufactured by ORTEC/AMTEK
 - Operated in a PopTop cryostat



[13]



[1]

- Each signal is a sequence of voltages sampled at a fixed interval
 - Observed noise levels after preprocessing reflect energy of pulse; signal-to-noise ratio (SNR)
 - Different rise times reflect different positions

Datasets: real detector data

Americium-241 source

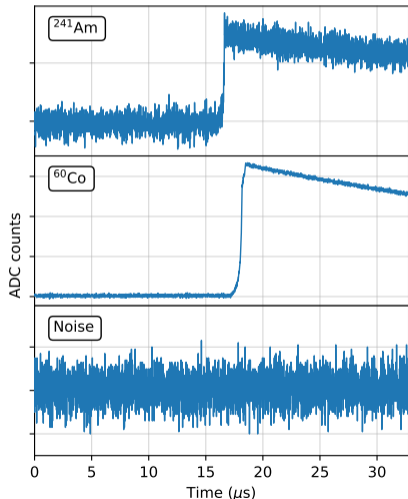
- Produces 60 keV γ s
- Almost entirely single-site events
- Lower energy (higher noise), good for *validation*

Cobalt-60 source

- Produces 1173 keV and 1332 keV γ s
- Numerous multi-site events from Compton scatters
- Higher energy (lower noise), good for *training*

Detector noise

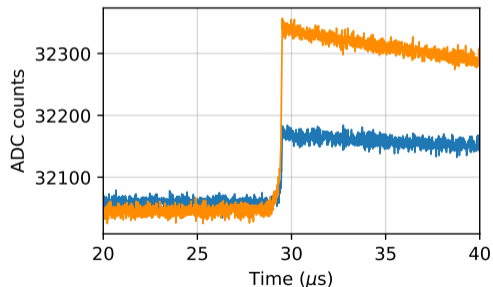
- Collected by randomly triggering the detector (and removing actual signals that occasionally occur)
- Used for *data augmentation*



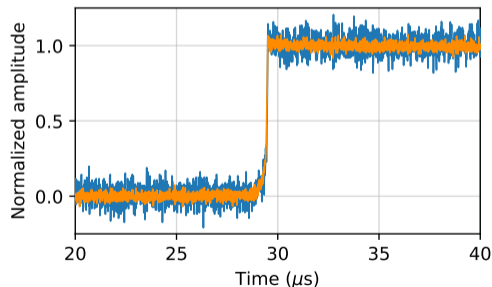
Datasets: real detector data (preprocessing)

- Data pulses preprocessed to remove baseline
- Data pulses have exponential decay removed with pole zero correction
- Data pulses scaled by amplitude (calculated with a trapezoidal filter)

Amplitude
normalization

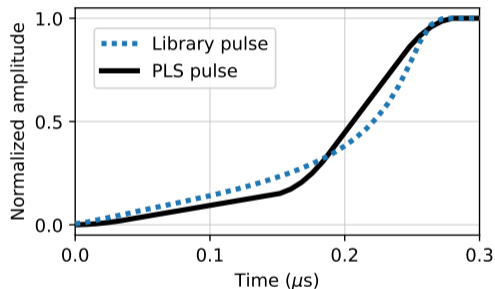


Before preprocessing



After preprocessing

Datasets: simulated data



[1]

Library pulses

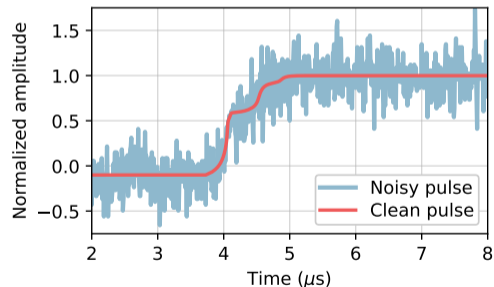
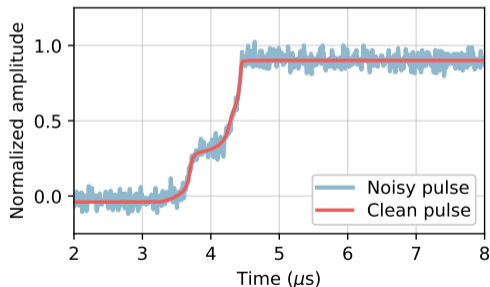
- 1724 simulated “library” pulses^[14]
- Each pulse corresponds to point on $1\text{ mm} \times 1\text{ mm}$ azimuthally symmetric grid
- Created using `siggen` simulation software^[15]
- Used to infer position of real events

Piecewise linear smoothed (PLS) pulses

- Mimic the general shape of the library pulses without the requirement of complex physics simulations

Datasets: simulated data (data augmentation)

- From the simulated single-site event pulses, can create a diverse training set
 - Combine single-site simulated pulses to create *artificial multi-site events*
 - Apply random *horizontal shifts*, *vertical shifts*, and *amplitude scales* to each pulse
 - Add *detector noise* to each pulse with a random standard deviation



Note: no preprocessing required for simulated pulses!

Training procedures

Regular

- Trained to map the noisy pulse to the corresponding clean underlying pulse
- Must know the true pulse – *only works on simulated data*

Noise2Noise^[16]

- Trained to map noisy pulse to noisy pulse (different noisy realizations of same underlying signal)
 - An impossible task in practice
 - Model will instead learn to predict the mean, given infinite different noisy realizations
- Can be used with simulations, *but this is not required*
 - For detector data, add even more noise to the already noisy pulse
 - Include a *total variation* penalty^[17] to original loss function L_0 to account for the noisy true mean
 - Penalize the absolute difference between given sample (j) and subsequent sample ($j + 1$) in pulse
 - Apply scaling factor λ to control weighting

$$L = L_0 + \frac{\lambda}{N} \sum_i^N \sum_j^{M-1} |z_{i,j+1} - z_{i,j}|$$

Training procedures

Regular

- Trained to map the noisy pulse to the corresponding clean underlying pulse
- Must know the true pulse – *only works on simulated data*

Noise2Noise^[16]

- Trained to map noisy pulse to noisy pulse (different noisy realizations of same underlying signal)
 - An impossible task in practice
 - Model will instead learn to predict the mean, given infinite different noisy realizations
- Can be used with simulations, *but this is not required*
 - For detector data, add even more noise to the already noisy pulse
 - Include a *total variation* penalty^[17] to original loss function L_0 to account for the noisy true mean
 - Penalize the absolute difference between given sample (j) and subsequent sample ($j + 1$) in pulse
 - Apply scaling factor λ to control weighting

$$L = L_0 + \frac{\lambda}{N} \sum_i^N \sum_j^{M-1} |z_{i,j+1} - z_{i,j}|$$

Training procedures

Regular

- Trained to map the noisy pulse to the corresponding clean underlying pulse
- Must know the true pulse – *only works on simulated data*

Noise2Noise^[16]

- Trained to map noisy pulse to noisy pulse (different noisy realizations of same underlying signal)
 - An impossible task in practice
 - Model will instead learn to predict the mean, given infinite different noisy realizations
- Can be used with simulations, *but this is not required*
 - For detector data, add even more noise to the already noisy pulse
 - Include a *total variation* penalty^[17] to original loss function L_0 to account for the noisy true mean
 - Penalize the absolute difference between given sample (j) and subsequent sample ($j + 1$) in pulse
 - Apply scaling factor λ to control weighting

$$L = L_0 + \frac{\lambda}{N} \sum_i^N \sum_j^{M-1} |z_{i,j+1} - z_{i,j}|$$

Training procedures

Regular

- Trained to map the noisy pulse to the corresponding clean underlying pulse
- Must know the true pulse – *only works on simulated data*

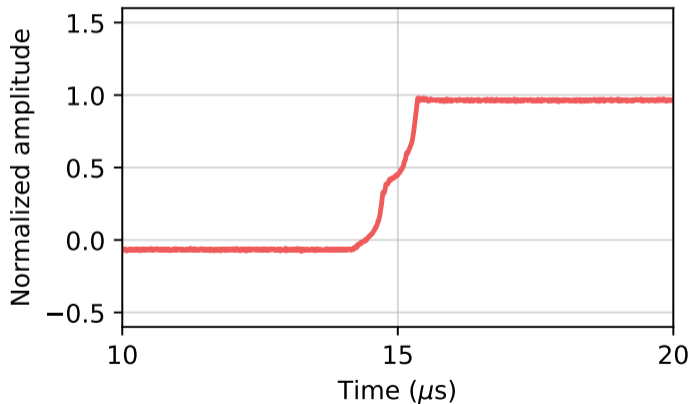
Noise2Noise^[16]

- Trained to map noisy pulse to noisy pulse (different noisy realizations of same underlying signal)
 - An impossible task in practice
 - Model will instead learn to predict the mean, given infinite different noisy realizations
- Can be used with simulations, *but this is not required*
 - For detector data, add even more noise to the already noisy pulse
 - Include a *total variation* penalty^[17] to original loss function L_0 to account for the noisy true mean
 - Penalize the absolute difference between given sample (j) and subsequent sample ($j + 1$) in pulse
 - Apply scaling factor λ to control weighting

$$L = L_0 + \frac{\lambda}{N} \sum_i^N \sum_j^{M-1} |z_{i,j+1} - z_{i,j}|$$

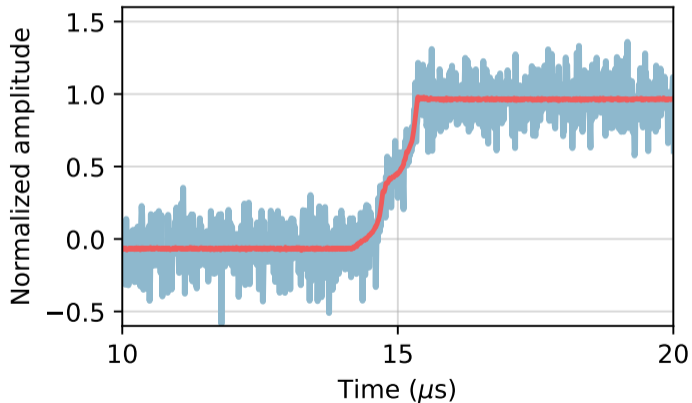
Noise2Noise

Original ^{60}Co data pulse (low noise/high energy/large SNR)



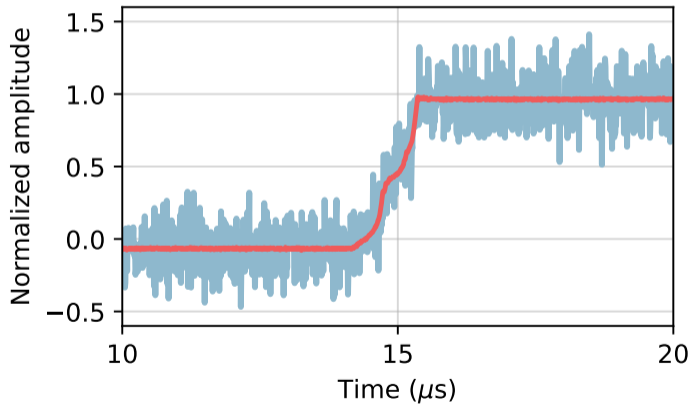
Noise2Noise

Original ^{60}Co data pulse with a random noise pulse

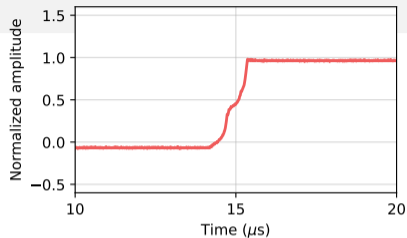


Noise2Noise

Original ^{60}Co data pulse with *another* random noise pulse

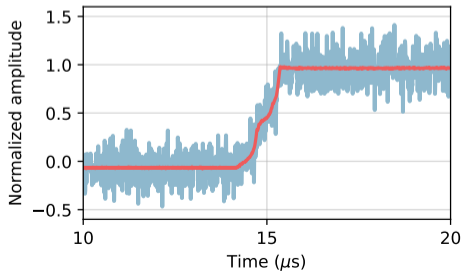
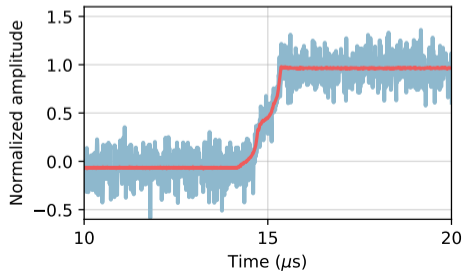


Noise2Noise



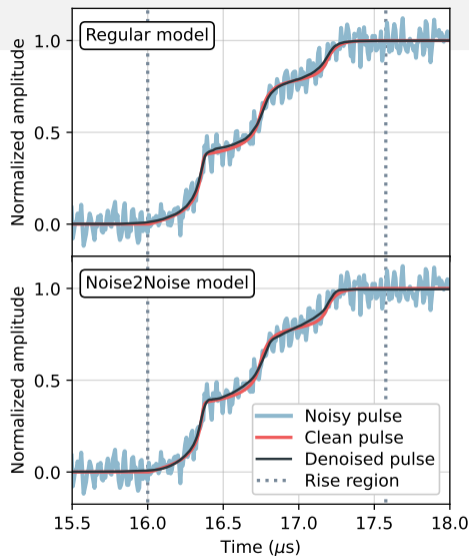
Input pulse

Target pulse



Results: simulations

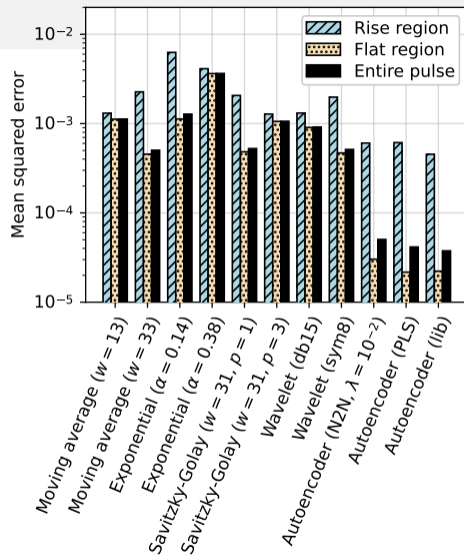
- Qualitatively, denoising with deep learning performs very well on simulations
- Autoencoder is superior to all traditional denoising methods investigated
 - Compared mean squared error on test set containing simulated single-/multi-site events
 - Each method optimized on a separate validation set to select hyperparameters
- Regular training procedure (simulations) outperforms Noise2Noise (^{60}Co data)
 - Still very good performance with Noise2Noise



[1] (modified)

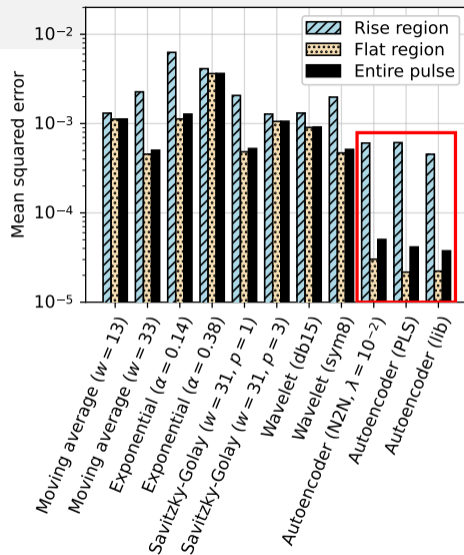
Results: simulations

- Qualitatively, denoising with deep learning performs very well on simulations
- Autoencoder is superior to all traditional denoising methods investigated
 - Compared mean squared error on test set containing simulated single-/multi-site events
 - Each method optimized on a separate validation set to select hyperparameters
- Regular training procedure (simulations) outperforms Noise2Noise (⁶⁰Co data)
 - Still very good performance with Noise2Noise



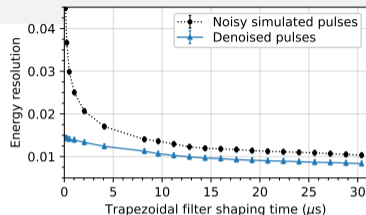
Results: simulations

- Qualitatively, denoising with deep learning performs very well on simulations
- Autoencoder is superior to all traditional denoising methods investigated
 - Compared mean squared error on test set containing simulated single-/multi-site events
 - Each method optimized on a separate validation set to select hyperparameters
- Regular training procedure (simulations) outperforms Noise2Noise (⁶⁰Co data)
 - Still very good performance with Noise2Noise

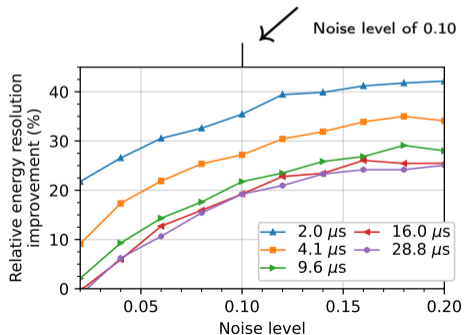


Results: simulations (energy resolution)

- In terms of physics results, allows for an improvement in the energy resolution
 - Energy calculated from the amplitude of a trapezoidal filter with given shaping time
 - FWHM of peak is the energy resolution
- Created test datasets with different noise levels and evaluated the energy resolution of each
- At every noise level and shaping time, the results after denoising with our autoencoder are superior
 - Proportionally larger improvements with increasing noise level, decreasing shaping time



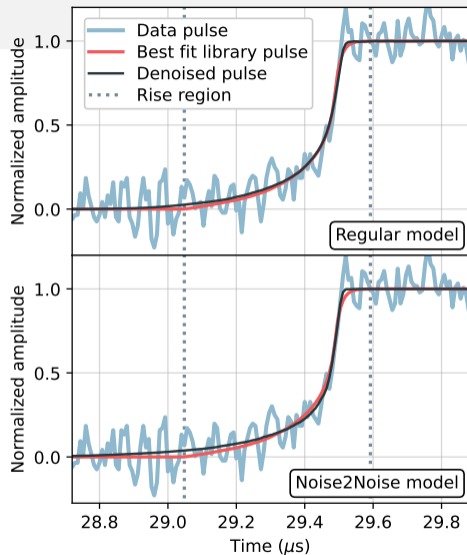
[1]



[1]

Results: data

- Qualitatively, denoising with deep learning performs very well on data
- More difficult to quantify denoising
 - No true underlying pulse to compare to
- However, can make a statistical comparison to evaluate the performance



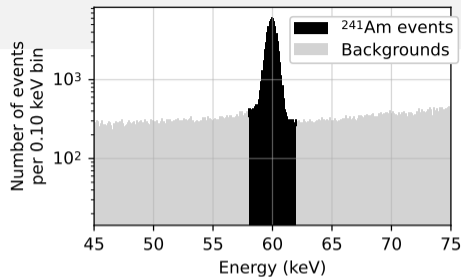
[1] (modified)

Results: data (χ^2 comparison)

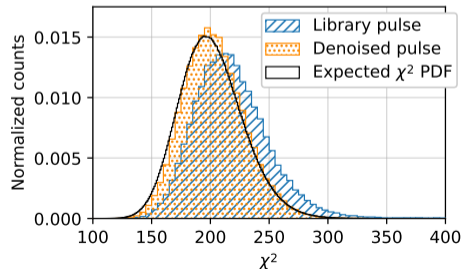
- ^{241}Am dataset contains mostly single-site events from 60 keV γ s
- Use a χ^2 comparison between the original pulse and **denoised pulse**, **best-fit library pulse**

$$\chi^2(x_i, z_i) = \sum_{j=M_1}^{M_2} \frac{(z_{i,j} - x_{i,j})^2}{\sigma_i^2}$$

- χ^2 distribution between noisy and **denoised pulse** is consistent with expected χ^2 distribution of our detector noise
 - Taken over 200 samples containing rise region (M_1, M_2 set appropriately)



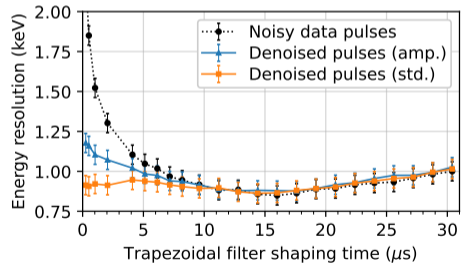
[1]



[1]

Results: data (energy resolution)

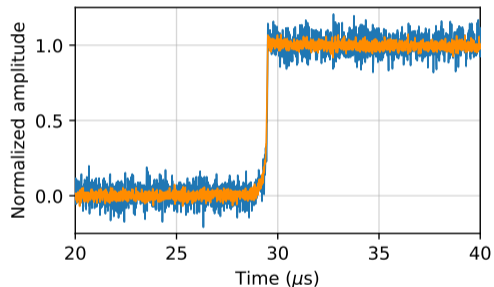
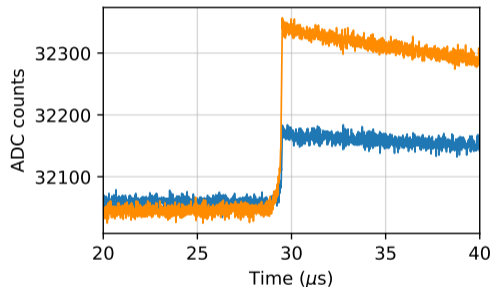
- Can also evaluate the effect of denoising on the energy resolution, compare to simulations
- Using ^{241}Am data, optimal energy resolution is comparable before and after denoising
- Much lower shaping time required to achieve good energy resolution
 - Important for data storage, analysis, etc.
- However, results are not as good as simulations would suggest
 - What's different?



[1]

Results: data (energy resolution)

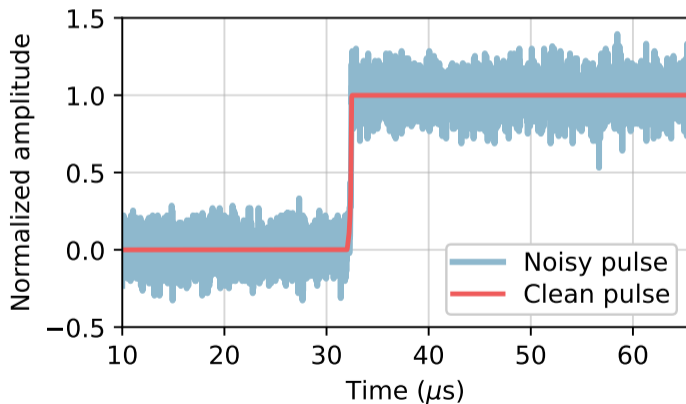
- We assume data pulses have *one* exponential decay and correct for that



- In reality, there are *multiple* sources of exponential decay, usually small, but still contribute
- A single “effective” pole zero correction is thus imperfect and leaves residual effects from the other exponential decays

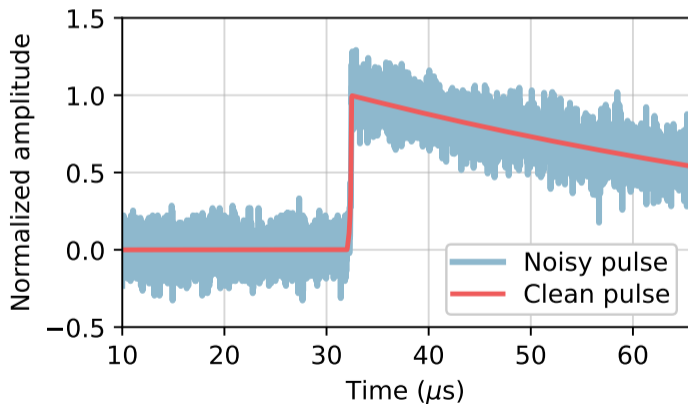
Results: data (energy resolution)

Simulated pulse with noise



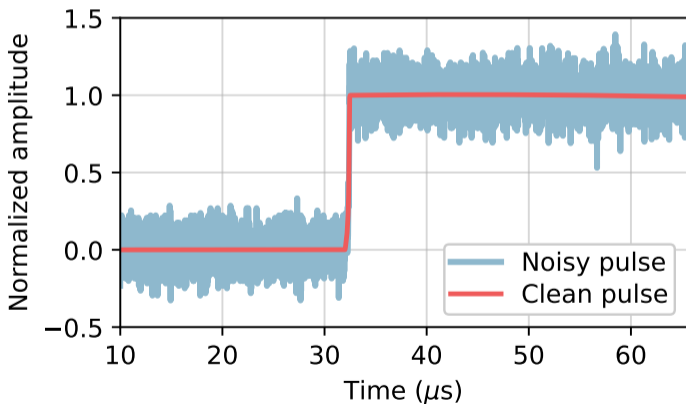
Results: data (energy resolution)

Simulated pulse with noise (convolved with multiple exponentials)



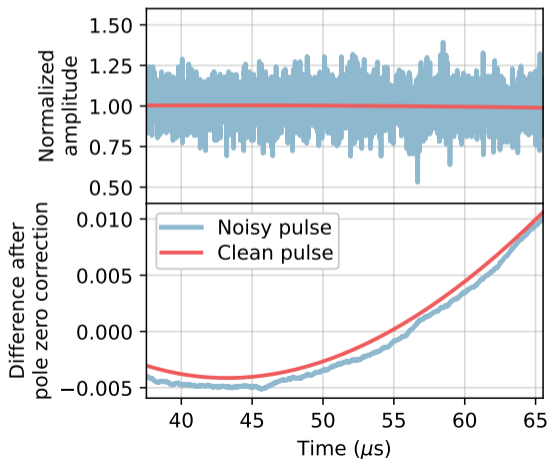
Results: data (energy resolution)

Simulated pulse with noise (deconvolved with one “effective” exponential)



Results: data (energy resolution)

Simulated pulse with noise (deconvolved with one “effective” exponential)



Conclusions and future work

- Deep convolutional autoencoders are effective at removing electronic noise from HPGe detector pulses
 - Outperforms various traditional denoising methods
 - Denoised pulses are statistically consistent with data pulses
 - Can reach optimal energy resolution with a lower shaping time
 - Simulations suggest improvements in the overall optimal energy resolution are possible
 - Accounting for effects present in real data could improve results
- Models can be trained *without* the need for detailed detector simulations
 - PLS pulses are a very rough approximation to library pulses
 - Noise2Noise method requires *only* noisy detector data
 - Results could likely be improved with more (diverse) data

Conclusions and future work

- Results presented here are focused on HPGe detector data
 - Noise removal is beneficial in many contexts
 - Our group is applying these methods to signals from other detector technologies
 - Gaseous proportional counters (e.g., see [talk from Noah Rowe](#)), bubble chambers
- Our group is also exploring various extensions of this research
 - New network architectures such as CycleGAN^[18] for improved performance
 - Potential to improve modelling of multiple exponential decays, and thus energy resolution, due to the less stringent requirement of unpaired simulated and detector pulses
 - Continuous inline denoising before triggering to reduce trigger thresholds
 - Useful to identify low SNR events otherwise dominated by electronic noise
- Work is broadly applicable to the particle astrophysics community and has great potential to be expanded on

Thank You!

More details in the published paper.
Check it out!

doi:[10.1140/epjc/s10052-022-11000-w](https://doi.org/10.1140/epjc/s10052-022-11000-w)

arXiv:[2204.06655](https://arxiv.org/abs/2204.06655)



Acknowledgements

- Thanks to all other authors of the paper
 - V. Basu, R. D. Martin, C. Z. Reed, N. J. Rowe, M. Shafiee, T. Ye
- This work was supported by the Natural Sciences and Engineering Research Council of Canada, the Arthur B. McDonald Canadian Astroparticle Physics Research Institute, and the Canada Foundation for Innovation
- The author held a Walter C. Sumner Memorial Fellowship



References I

- [1] M. R. Anderson *et al.*, “Performance of a convolutional autoencoder designed to remove electronic noise from p-type point contact germanium detector signals,” *Eur. Phys. J. C*, vol. 82, no. 12, p. 1084, 2022.
- [2] S. I. Alvis *et al.*, “Search for neutrinoless double- β decay in ^{76}Ge with 26 kg – yr of exposure from the Majorana Demonstrator,” *Phys. Rev. C*, vol. 100, p. 025501, 2019.
- [3] M. Agostini *et al.*, “Final results of GERDA on the search for neutrinoless double- β decay,” *Phys. Rev. Lett.*, vol. 125, p. 252502, 2020.
- [4] N. Abgrall *et al.*, “LEGEND-1000 preconceptual design report,” *arXiv preprint arXiv:2107.11462*, 2021.
- [5] C. E. Aalseth *et al.*, “CoGeNT: A search for low-mass dark matter using p-type point contact germanium detectors,” *Phys. Rev. D*, vol. 88, no. 1, p. 012002, 2013.
- [6] M. Agostini *et al.*, “First search for bosonic superweakly interacting massive particles with masses up to $1\text{ MeV}/c^2$ with GERDA,” *Phys. Rev. Lett.*, vol. 125, no. 1, p. 011801, 2020.
- [7] N. Abgrall *et al.*, “Search for Pauli Exclusion Principle violating atomic transitions and electron decay with a p-type point contact germanium detector,” *Eur. Phys. J. C.*, vol. 76, no. 11, pp. 1–5, 2016.

References II

- [8] S. I. Alvis *et al.*, “First limit on the direct detection of lightly ionizing particles for electric charge as low as $e/1000$ with the Majorana Demonstrator,” *Phys. Rev. Lett.*, vol. 120, no. 21, p. 211804, 2018.
- [9] S. I. Alvis *et al.*, “Search for trinucleon decay in the Majorana Demonstrator,” *Phys. Rev. D*, vol. 99, no. 7, p. 072004, 2019.
- [10] “Underground neutrino experiment could provide greater clarity on matter-antimatter imbalance,” accessed: 2023-05-13. [Online]. Available: <https://newscenter.lbl.gov/2018/03/26/neutrino-experiment-probes-matter-antimatter-imbalance/>
- [11] “Building autoencoders in keras,” accessed: 2023-05-13. [Online]. Available: <https://blog.keras.io/building-autoencoders-in-keras.html>
- [12] P. Vincent, H. Larochelle, I. Lajoie, Y. Bengio, and P.-A. Manzagol, “Stacked denoising autoencoders: Learning useful representations in a deep network with a local denoising criterion,” *J. Mach. Learn. Res.*, vol. 11, no. Dec, pp. 3371–3408, 2010.
- [13] “P-type point-contact (PPC) germanium detectors,” accessed: 2023-05-13. [Online]. Available: <https://www.npl.washington.edu/majorana/design-technologies>

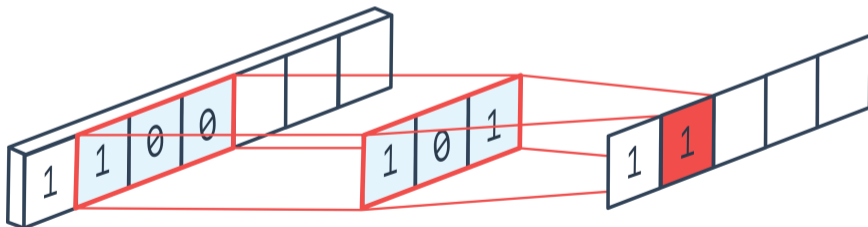
References III

- [14] Vasundhara, "Pulse fitting for event localization in high purity germanium point contact detectors," Master's thesis, Queen's University, 2020.
- [15] D. C. Radford, "sigen," 2017. [Online]. Available: https://github.com/radforddc/icpc_sigen
- [16] J. Lehtinen *et al.*, "Noise2Noise: Learning image restoration without clean data," in *Proc. Int. Conf. Mach. Learn.*, vol. 80, 2018, pp. 2965–2974.
- [17] L. I. Rudin, S. Osher, and E. Fatemi, "Nonlinear total variation based noise removal algorithms," *Physica D*, vol. 60, no. 1-4, pp. 259–268, 1992.
- [18] J.-Y. Zhu, T. Park, P. Isola, and A. A. Efros, "Unpaired image-to-image translation using cycle-consistent adversarial networks," in *Proc. IEEE Int. Conf. Comput. Vis.*, 2017, pp. 2223–2232.
- [19] "1D convolution," accessed: 2022-08-10. [Online]. Available: <https://peltarion.com/knowledge-center/documentation/modeling-view/build-an-ai-model/blocks/1d-convolution>
- [20] "Med Phys 4RA3, 4RB3/6R03 - Chapter 6: Pulse Processing," accessed: 2023-05-13. [Online]. Available: https://www.science.mcmaster.ca/radgrad/images/6R06CourseResources/4RA34RB3_Lecture_Note_6_Pulse-Processing.pdf

Additional Slides

Model architecture

- Fully convolutional autoencoder
 - Weight sharing provides consistent noise removal across pulse
 - Feature locality and shift equivariance
 - Allows for a variable input shape (subject to some restrictions)
 - Significant reduction in the number of trainable parameters



[19]

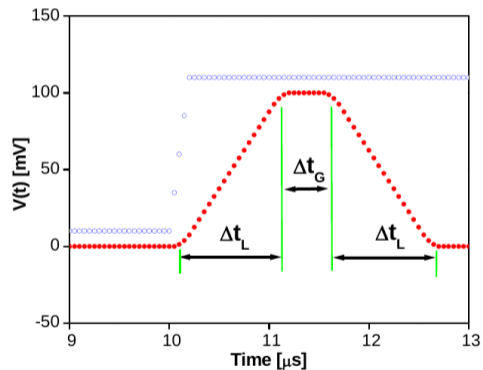
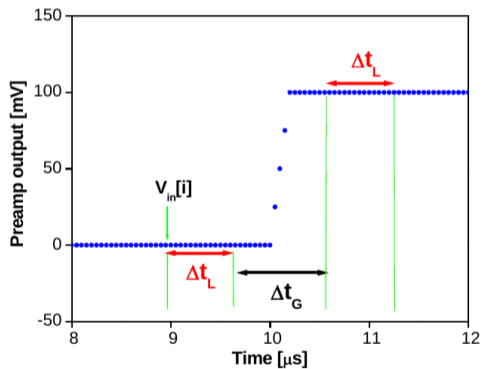
Model architecture

| Layer | Stride | Window | Output |
|-----------------------|--------|--------|----------|
| Input | | | 4096, 1 |
| Convolution | 1 | 1 | 4096, 8 |
| Convolution | 1 | 9 | 4088, 16 |
| Average Pooling | 2 | 2 | 2044, 16 |
| Convolution | 1 | 17 | 2028, 32 |
| Average Pooling | 2 | 2 | 1014, 32 |
| Convolution | 1 | 33 | 982, 64 |
| Average Pooling | 2 | 2 | 491, 64 |
| Convolution | 1 | 33 | 459, 32 |
| Transpose Convolution | 1 | 33 | 491, 32 |
| Upsampling | 2 | 2 | 982, 64 |
| Transpose Convolution | 1 | 33 | 1014, 64 |
| Upsampling | 2 | 2 | 2028, 64 |
| Transpose Convolution | 1 | 17 | 2044, 32 |
| Upsampling | 2 | 2 | 4088, 32 |
| Transpose Convolution | 1 | 9 | 4096, 16 |
| Convolution (output) | 1 | 1 | 4096, 1 |

Results on simulations

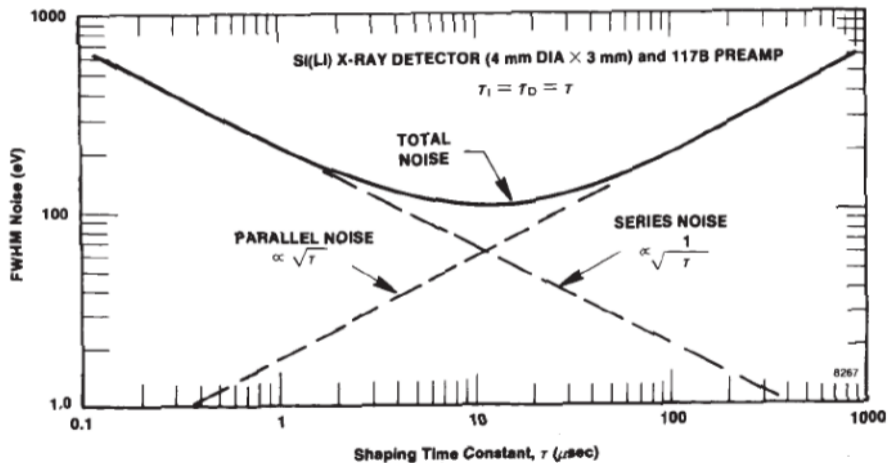
| Training procedure and data | | | Mean squared error ($\times 10^{-5}$) | | | |
|-----------------------------|----------|----------|---|------|----------------|------|
| Procedure | Data | Noise | Gaussian noise | | Detector noise | |
| | | | Library | PLS | Library | PLS |
| Regular | Library | Detector | 4.12 | 4.72 | 3.76 | 4.21 |
| Regular | Library | Gaussian | 3.40 | 3.82 | 4.50 | 4.77 |
| Regular | PLS | Detector | 5.10 | 4.48 | 4.15 | 3.57 |
| Regular | PLS | Gaussian | 3.93 | 3.36 | 5.02 | 4.31 |
| N2N ($\lambda = 0$) | Library | Detector | 3.90 | 4.37 | 3.86 | 4.20 |
| N2N ($\lambda = 0$) | Library | Gaussian | 3.46 | 3.87 | 4.57 | 4.82 |
| N2N ($\lambda = 0$) | PLS | Detector | 5.11 | 4.48 | 4.14 | 3.55 |
| N2N ($\lambda = 0$) | PLS | Gaussian | 3.85 | 3.46 | 4.97 | 4.43 |
| N2N ($\lambda = 0$) | Detector | Detector | 6.54 | 6.30 | 7.78 | 7.40 |
| N2N ($\lambda = 10^{-2}$) | Detector | Detector | 4.17 | 4.54 | 5.04 | 5.26 |

Trapezoidal filter

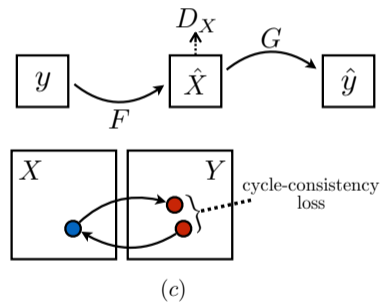
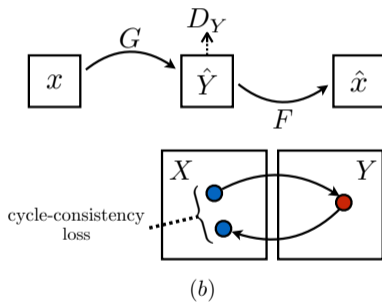
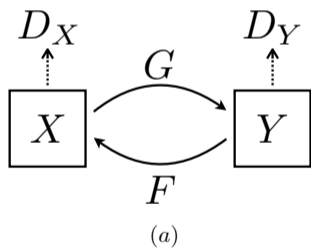


[20]

Noise curve



CycleGAN



[18]